Food Science of Animal Resources

Food Sci. Anim. Resour. 2023 September 43(5):840~858
DOI https://doi.org/10.5851/kosfa.2023.e39

pISSN : 2636-0772 eISSN : 2636-0780
http://www.kosfaj.org

ARTICLE

Quality Evaluation of Mackerel Fillets Stored under Different Conditions by Hyperspectral Imaging Analysis

Azfar Ismail[1,2], Jiwon Ryu[3,4], Dong-Gyun Yim[1], Ghiseok Kim[3,4], Sung-Su Kim[1], Hag Ju Lee[1], and Cheorun Jo[1,5,*]

[1]Department of Agricultural Biotechnology, Center for Food and Bioconvergence, and Research Institute of Agriculture and Life Science, Seoul National University, Seoul 08826, Korea
[2]Department of Aquaculture, Faculty of Agriculture, Universiti Putra Malaysia, Selangor 43400, Malaysia
[3]Department of Biosystems and Biomaterials Science and Engineering, Seoul National University, Seoul 08826, Korea
[4]Integrated Major in Global Smart Farm, College of Agriculture and Life Sciences, Seoul National University, Seoul 08826, Korea
[5]Institute of Green Bio Science and Technology, Seoul National University, Pyeongchang 25354, Korea

OPEN ACCESS

Received June 13, 2023
Revised July 18, 2023
Accepted July 20, 2023

***Corresponding author** : Cheorun Jo
Department of Agricultural Biotechnology, Center for Food and Bioconvergence, and Research Institute of Agriculture and Life Science, Seoul National University, Seoul 08826, Korea
Tel: +82-2-880-4804
Fax: +82-2-873-2271
E-mail: cheorun@snu.ac.kr

***ORCID**
Azfar Ismail
https://orcid.org/0000-0002-7095-9415
Jiwon Ryu
https://orcid.org/0000-0001-7927-9654
Dong-Gyun Yim
https://orcid.org/0000-0003-0368-2847
Ghiseok Kim
https://orcid.org/0000-0003-2177-0031
Sung-Su Kim
https://orcid.org/0000-0002-8416-5026
Hag Ju Lee
https://orcid.org/0000-0003-2906-7666
Cheorun Jo
https://orcid.org/0000-0003-2109-3798

Abstract This study was designed to compare the quality changes in mackerel fillets stored under different conditions by using hyperspectral imaging (HSI) techniques. Fillets packaged in vacuum were stored for six days under five different conditions: refrigerated at 4°C (R group); iced at 5±3°C (I group); kept at an ambient of 17±2°C (A group); frozen at –18°C for 24 h and thawed in a refrigerator at 4°C for 5 h on the sampling day (FTR group); FTR thawed in tap water instead of thawing in a refrigerator (FTW group). The FTR group had the lowest total bacterial count, drip loss, 2-thiobarbituric acid reactive substances, volatile basic nitrogen, and texture profile analysis values among groups during the entire storage period ($p<0.05$). Scanning electron microscopy revealed that the FTR group had less damage, while the other groups had shrunken muscle tissues. HSI integrated with the partial least squares model yielded reliable and efficient results, with high R^2_{cv} values, for several quality parameters of the mackerel fillets. Overall, the FTR group, involving freezing and thawing in a refrigerator, appears to be the most favorable option for maintaining the quality of mackerel fillets, which could be practically implemented in the industry. HSI is a suitable and effective technique for determining the quality of mackerel fillets stored under different conditions.

Keywords mackerel fillets, optimal storage, freshness, frozen-thawed, hyperspectral imaging

Introduction

The freshness of muscle food, especially fish, is vital because it influences consumer

purchasing decisions. Fish are prone to quality deterioration owing to the rapid degradation of muscle tissues during the post-mortem period during (Hashimoto et al., 2017). Deterioration of fish quality results in organoleptic changes, such as discoloration and off-flavors, making it undesirable for human consumption. The freshness of fish is difficult to sustain for a longer period because of the high moisture and lipid contents, rapid enzymatic activity, neutral pH, and high microbial proteolysis in fish (Prabhakar et al., 2020; Zhou et al., 2021). Proteolytic activity in fish is affected by several factors such as temperature, muscle pH, water content, genetics, nutrition, age, and gender (Matarneh et al., 2017; Singh and Benjakul, 2018).

Among storage methods, freezing is the preferred technique to maintain quality for extended preservation of fish freshness because low temperatures slow down proteolysis and endogenous enzyme activities in muscle food (Chan et al., 2020; Roiha et al., 2018). Thus, the freezing method protects fish tissues from rapid degradation by biological, chemical, and physical processes, such as bacterial growth, oxidation, and dehydration, maintaining their flavor and nutritional value (Duarte et al., 2020; Hassoun et al., 2020; Huang et al., 2021). In contrast, high freezing temperatures trigger proteolytic enzyme activities, decreasing the tenderness and increasing the spoilage of fish (Kaur et al., 2021). High ambient storage temperature (10℃–25℃) results in rapid degradation of fish quality compared to freezing and refrigerating conditions (Chen et al., 2021; Khoshnoudi-Nia and Moosavi-Nasab, 2019). Ice chilling is the traditional method of storage at low temperatures. However, this is not practically applied in the supply chain and long term storage, because the introduction of cooling technology and the use of ice incurs extra costs for controlling the storage temperature (Cropotova et al., 2019; Magnussen et al., 2008). Therefore, the impact of various storage conditions on the thorough information of quality and shelf life of fish should be assessed.

Hyperspectral imaging (HSI) has been introduced in food quality evaluation to replace conventional methods, which are time-consuming, expensive, and susceptible to large sources of variation (Hassoun and Karoui, 2017). HSI is a non-destructive spectral method with effective and accurate quality detection abilities (Wu et al., 2018). It extracts spectral and spatial information by absorbing, transmitting, reflecting, and scattering images of food products (Cheng et al., 2017). HSI acquires information on the quality of fishery products in each pixel from different locations without affecting sample integrity (Chen et al., 2021; Govari et al., 2021; Khoshnoudi-Nia and Moosavi-Nasab, 2019; Moosavi-Nasab et al., 2021; Temiz and Ulaş, 2021). However, none of the studies conducted thoroughly compared the physical, chemical, and biological characteristics of fish fillets using the HSI tool. This study aimed to compare the quality changes in mackerel fillets stored under different conditions using conventional and HSI techniques to investigate the potential of HSI for rapid prediction of physicochemical traits in fish. By incorporating fundamental HSI processing, valuable insights can be gained to practically implement in the short-chain supply before reaching consumers.

Materials and Methods

Raw material and experimental design

A total of 96 live chub mackerels (Scombus japonicus), typically ranging in size from 23 to 35 cm and weighing around 200 to 300 g, with approximately 24 months of age, were purchased from the fish market in Incheon, Korea, and transferred to the laboratory. Chub mackerel was chosen because it is a good source of omega-3 fatty acids and is widely distributed in various regions, including the western Pacific Ocean, the eastern Atlantic Ocean, and the Mediterranean Sea. After stunning, the mackerels were filleted and stored at 4℃ for 8 hours to allow rigor mortis to set in. Approximately 150 g of the sample was vacuumed and packaged (HFV-600L, Hankook Fujee Machinery, Hwaseong, Korea) in low-density polyethylene/nylon bags (0.09 mm thickness; O_2 permeability of 2 mL/m^2/d at 0℃; Sunkyung, Seoul, Korea). Mackerel fillets were stored for six

days using five different methods: refrigerated at 4℃ (R group); iced at 5±3℃ (I group); kept at an ambient temperature of 17±2℃ (A group); frozen at –18℃ for 24 h and thawed in a refrigerator at 4℃ for 5 h on the sampling day (FTR group); FTR thawed in tap water instead of in a refrigerator (FTW group). Each group had three replicates. Fillets were analyzed on days 1, 3, and 6 of storage. Approximately 10×5×3 cm fillets (n=6) were cut for HSI analysis in both sides, while the remaining fillets underwent immediate laboratory analysis or were ground and kept at –20℃ until analysis.

Chemical analyses

pH content

One gram of each sample was homogenized with 9 mL distilled water using a homogenizer (Ultra-Turrax T25, Ika-Werke, Staufen, Germany) at 1,720×g for 30 s. The homogenates were centrifuged (Union 32R, Hanil, Seoul, Korea) at 2,265×g for 10 min and filtered (Whatman No. 4, Whatman plc, Maidstone, UK). The pH of each filtrate was measured using a pH meter (SevenGo, Mettler-Toledo, Schwerzenbach, Switzerland).

Total bacterial count (TBC)

TBC was performed according to the ICMSF (1986) by aseptically transferring 10 g of the sample to a sterile bag containing 90 mL of saline solution. After mixing, serial dilutions (10^1 to 10^4 Log CFU/g) of the samples were prepared. Then, 100 μL aliquots of appropriate dilutions were spread on plate count agar, incubated at 37℃ for 48–72 h, and then colonies were counted.

Volatile basic nitrogen (VBN)

Protein oxidation was assessed based on the VBN value obtained using the Conway micro-diffusion technique (Conway, 1947). Three grams of sample was homogenized with 27 mL of distilled water using a homogenizer (Ultra-Turrax T25, Ika-Werke) at 1,720×g for 30 s. The homogenates were centrifuged (Union 32R, Hanil) at 2,265×g for 10 min and filtered (Whatman No. 1, Whatman plc). Subsequently, 1 mL each of the sample, 50% K_2CO_3, and 0.01N H_3BO_3 and 100 μL indicator (0.066% methyl red in ethanol: 0.066% bromocresol green in ethanol, 1:1, w/v) were poured into the Conway. Color changes were observed and recorded by adding 0.01 N HCl to the center of the Conway.

2-Thiobarbituric acid reactive substances (TBARS) value

Lipid oxidation was measured using the TBARS assay following the process described by (Lee et al., 2016), with a slight modification. Five grams of sample were homogenized with 9 mL of distilled water and 50 μL of 2% tert-butyl-4-hydroxyanisole ethanol solution (BHT) using a homogenizer (Ultra-Turrax T25, Ika-Werke) at 1,720×g for 30 s. The homogenates were centrifuged (Union 32R, Hanil) at 2,265×g for 15 min and filtered (Whatman No. 1, Whatman plc). The supernatants (2 mL) were mixed with 4 mL of thiobarbituric-trichloroacetitic acid solution. The homogenates were then heated in a water bath at 90℃ for 30 min and cooled. Subsequently, 300 μL of the supernatant was placed into a microplate, and the absorbance was measured at 532 nm using a spectrophotometer (X-ma 3100, Human, Gwangju, Korea).

Drip loss

Mackerel fillets were weighed before and after storage. The samples were wiped using a clean tissue before weighing. Drip loss was determined as the percentage ratio of the removed weight to the initial weight of the sample.

Water content

Three grams of each sample were distributed into an aluminum dish. The samples were then oven dried at 110℃ for 16 h. The difference in weight before and after oven drying was recorded as a percentage.

Color

Color parameters were measured using a colorimeter (CR-400 Chroma Meter, Konica Minolta, Osaka, Japan) calibrated with a white standard plate (International Commission of Illumination; CIE L*=96.79, CIE a*=0.30, and CIE b*=1.67). The surfaces of the samples were analyzed six times. There were two types of muscles measured for color: dark muscles, characterized by brown or reddish tissue on the flesh from the presence of myoglobin pigmentation, and white muscles, which exhibited white to off-white tissue on the flesh due to the lower levels of myoglobin. The results were presented as CIE L*, CIE a*, and CIE b*.

Texture profile analysis

The texture profile was analyzed using a TA1 texture analyzer (AMETEK Lloyd Instruments, Fareham, UK). Ten grams of ground sample was placed into a petri dish (35×10 mm^2), cooked in a laboratory water bath at 80℃ for 20 min, and cooled. A compression plate of Ø 70 mm was attached to the analyzer that compressed the samples twice (test speed of 2 mm/s, maximum cell load 50 kg, compression level 60%, and trigger force of 0.1 N). The data were analyzed using the NexygenPlus software program (AMETEK Lloyd Instruments) with the following parameters: hardness (N) represents the maximum force required to compress the sample; springiness (mm) refers to the duration ability of the sample to recover its original form after a deforming force has been removed; chewiness (N) is the work required to chew or crunch the sample for swallowing; cohesiveness (N) indicates the extent of total energy required to which the sample can be deformed prior to rupture; adhesiveness (kgf.mm) is the work necessary to pull the compressing plunger away from the sample, represented by the negative area under the baseline between the compression cycles; elasticity represents the ability of sample to regain its original shape or structure after deformation or compression, and gumminess (N) indicates the force necessary to disintegrate a semi-solid sample for swallowing (Bourne, 2002).

Scanning electron microscope (SEM) observation

SEM was conducted according to the method described by Andrés et al. (2006), with some modifications. The sample (0.5×0.4×0.3 cm^3) was fixed with Carnoy's solution at 4℃ for 24 h. The samples were then dehydrated using ethyl alcohol and immersed in hexamethyldisilazane for 10 min. The dried sample was mounted on an aluminum stub with carbon tape. It was then thinly coated with platinum under vacuum pressure (EM ACE200, Leica, Wetzlar, Germany). The samples were observed under a field-emission SEM (SUPRA 55VP, Carl Zeiss, Oberkochen, Germany).

Hyperspectral imaging (HSI) analysis

Hyperspectral imaging (HSI) system and data acquisition

HSI analysis was performed using a push broom scanner with an HSI-200 sensor (Korea Spectral Products, Seoul, Korea). Each pixel of an image consisted of 640 wavelengths of the spectrum covering the wavelength region from 400 to 1,700 nm. Ninety-six samples of mackerel fillets were observed using HSI, which indicates two sides of the fillets; inside (Fig. 1A) and

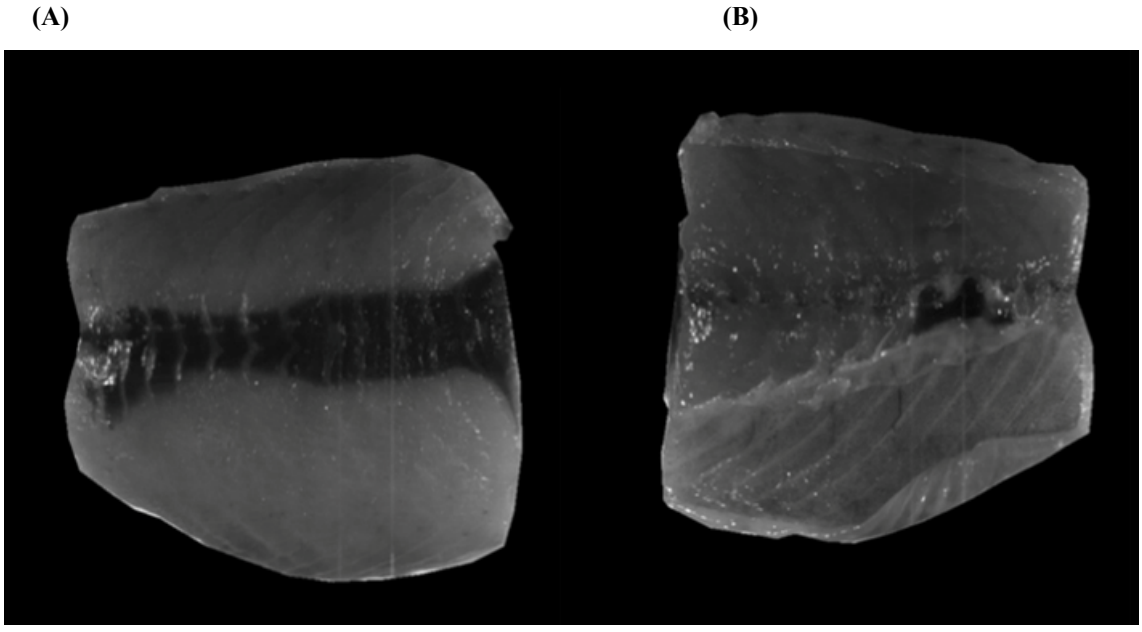

Fig. 1. The fillets near the skin (A) and the fillets near the internal organs (B) of mackerel from hyperspectral images.

outside (Fig. 1B). However, the average data was tabulated at only inside of the fish fillets to obtain a better predict information with less variation in each region of interest (RoI). HSI was equipped with an imaging spectrometer with a resolution of 640 spectral x 512 spatial generated using a InGaAs PIN-Photodiode hyperspectral camera in the spectral range of visible and short-wave near-infrared regions.

The white reference was acquired using a Teflon whiteboard (99.99% reflectivity), and the dark reference was acquired by covering the camera (0% reflectance). This was done to eliminate the dark current effect and reduce the influence of uneven illumination, resulting in small ranged from 0 to 1. Normalized reflectance data were calculated using Eq. (1). After constructing the reflectance data, each spectrum included in the RoI of the same sample was averaged into a single spectrum for analysis.

$$Normalized\ \ reflectance = \frac{Reflectance\ \ value}{Reference\ \ reflectance\ \ value} \times scale\ \ factor \quad (1)$$

Data processing method

To minimize the noise from the raw reflectance data, only the spectra from 750 to 1,300 nm were used for the analysis. To remove unnecessary baseline drifts among the signals, all signals were scaled into the range of 0 to 1 (min-max normalization). The reflectance spectra were recorded by indicating the raw data and signals after pre-processing.

Partial least square (PLS) was used to construct data for analysis and modelling. A comparison was made between the hyperspectral data and twenty-eight different quality parameters of mackerel fillets (n=96), which revealed that 17 of these parameters yielded reliable results.

To enhance data processing performance, the leave-one-out cross-validation method was employed for calibration and validation of the PLS models according to the method by Xu et al. (2018). The optimal number of PLS components (N) for each quality parameter was determined based on the lowest value of the root-mean-square error estimated by cross-validation (RMSECV).

Statistical analysis

Data were analyzed by one-way ANOVA and Tukey's test at a significance level of 95% using SAS 9.4 program (SAS Institute, Cary, NC, USA). Data are presented as mean (n=3) and standard error of the mean. The PLS and principal component analysis (PCA) models of the entire HSI dataset of mackerel fillets (n=96) were implemented in Python version 3.7.9 (Python Software Foundation, Beaverton, OR, USA).

Results and Discussion

General quality properties

The FTR group showed significantly the lowest drip loss among the treatments on days 1 and 6 (Table 1). Significant water loss in the muscle and is lethal to bacterial growth due to the ice crystal formation (Cropotova et al., 2019; Tan et al., 2021). On day 1, drip loss was the highest in the FTW group (2.77%) compared to the other groups (0.51%–1.32%; $p<0.05$). Water content and pH are the major post-mortem changes in fish muscle due to the water loss or exudation occurring during muscle stiffening. These changes lead to an increase in rigidity, reaching a maximum level after 12 to 24 hours (Chan et al., 2020).

Table 1. Typical quality properties of mackerel fillets stored under different conditions

Trait	Storage method	Storage period (days)				SEM[1)]
		0	1	3	6	
Drip loss (%)	A	NA	0.57^{bz}	1.58^{a}	1.77^{ax}	0.069
	I	NA	1.32^{by}	2.17^{a}	2.03^{ax}	0.128
	R	NA	0.74^{bz}	1.50^{a}	1.57^{ax}	0.123
	FTW	NA	2.77^{ax}	1.27^{c}	1.95^{bx}	0.133
	FTR	NA	0.51^{z}	1.05	0.69^{y}	0.125
	SEM[2)]	NA	0.103	0.188	0.135	
Water content (%)	A	60.23	60.64	64.18^{x}	60.58	0.992
	I	60.23^{ab}	60.08^{ab}	61.52^{axy}	58.68^{b}	0.421
	R	60.23	59.56	61.01^{xy}	60.90	0.589
	FTW	60.23	58.31	60.79^{xy}	60.29	1.211
	FTR	60.23	58.70	59.62^{y}	59.01	1.452
	SEM[2)]	NA	0.639	0.722	0.792	
pH value	A	5.69^{c}	6.00^{b}	6.71^{a}	6.07^{b}	0.059
	I	5.69^{c}	6.01^{b}	6.61^{a}	6.14^{b}	0.034
	R	5.69^{c}	5.98^{b}	6.63^{a}	6.05^{b}	0.036
	FTW	5.69^{c}	6.01^{b}	6.69^{a}	6.03^{b}	0.030
	FTR	5.69^{c}	5.95^{c}	6.65^{a}	6.10^{b}	0.019
	SEM[2)]	NA	0.034	0.024	0.051	

[1)] n=3 of standard error of the least square mean.
[2)] n=15 of standard error of the least square mean.
[a–c] Different superscripts indicate significant difference among means ($p<0.05$).
[x–z] Different superscripts indicate significant difference among means ($p<0.05$).
A, ambient; I, ice; R, refrigerator; FTW, frozen and thawed in water; FTR, frozen and thawed in a refrigerator; NA, not applicable.

Temperature abuse during the thawing process leads to rapid changes in the water content of a previously frozen condition (Negara et al., 2021). The water content in group A increased within three days and then dropped on day 6 ($p>0.05$). Group A was exposed to ambient temperature, which caused muscle contraction and resulted in higher water content compared to other storage methods during three days of storage. Relative humidity of storage was fixed at 40% in all storage methods.

Theoretically, an increase in pH reflects an increase in the water content in the muscle protein via charge shielding (Brewer, 2014). However, no significant difference in pH was observed among the groups. When the autolytic processes were initiated, quality deterioration also started due to a favorable environment for bacterial growth (Duarte et al., 2020). Among the different groups, group I had the lowest pH (6.61) at 3 d and the highest pH on day 6 (6.14; $p>0.05$). This might be due to the effects of temperature on extracellular proteolysis and the increase in pH caused by bacterial accumulation (Toe et al., 2019). The increase in pH on day 3 may be due to post-rigor changes (Matarneh et al., 2017). The sudden decrease in pH on day 6 was due to the break down of muscle glycogen, producing lactic acid, which caused acidification and post-mortem softening of fish flesh (Liu et al., 2013; Singh and Benjakul, 2018).

Color represents the constituents of several compounds in muscle tissues. For instance, dark muscles have more prominent fat and myoglobin content than white muscles because of the higher amount of lipid droplets and myofibrillar protein in the tissues (Listrat et al., 2016). Table 2 shows the comparison of dark and white muscles in fish fillets stored using different methods. For CIE L*, no significant difference was found in dark muscles, except in the FTW group. The frozen mackerel was appeared to be darker after water thawing owing to water loss and destruction of the microstructure (Zhang et al., 2021). Zhou and Xie (2021) agreed that fish had better CIE L* after thawing in the refrigerator and temperature rise resulted in the worst color values because of protein denaturation.

CIE a* of muscle tissues is primarily influenced by the pigmentation of myoglobin (Greer, 2020). The FTR and FTW groups had lower CIE a* in the dark muscles compared to the other storage groups, which turned the fillets into purple-red due to deoxygenation, freezer burn, or abnormally long storage (Wang and Xie, 2020). In the white muscle, the CIE a* were contradictory to those of the dark muscle. This might be due to the low myoglobin content in the muscle, which affects color

Table 2. Color of dark muscles and white muscles of mackerel fillets stored under different conditions

Type of muscle	Item	Storage method	Storage period (days)				SEM[1)]
			0	1	3	6	
Dark muscle	CIE L*	A	44.91	40.62	44.41	42.36	1.637
		I	44.91	41.37	45.30	42.55	0.826
		R	44.91	41.70	41.46	41.62	1.504
		FTW	44.91^{a}	37.68^{b}	39.44^{b}	39.80^{b}	1.583
		FTR	44.91	43.70	41.13	43.84	1.248
		SEM[2)]	-	1.486	1.737	1.386	
	CIE a*	A	11.88	14.42^{xy}	12.84^{xy}	15.61^{x}	0.928
		I	11.88	16.36^{x}	15.01^{x}	16.51^{x}	0.639
		R	11.88	14.79^{bxy}	16.06^{ax}	16.99^{ax}	0.436
		FTW	11.88	13.41^{y}	11.24^{y}	10.70^{y}	0.826
		FTR	11.88^{b}	13.53^{ay}	12.90^{axy}	10.99^{by}	0.215
		SEM[2)]	-	0.510	0.986	0.402	

Table 2. Color of dark muscles and white muscles of mackerel fillets stored under different conditions (continued)

Type of muscle	Item	Storage method	Storage period (days)				SEM[1)]
			0	1	3	6	
Dark muscle	CIE b*	A	15.25^{c}	17.82^{ab}	17.42^{b}	19.47^{a}	0.408
		I	15.25^{b}	17.65^{ab}	18.44^{a}	18.59^{a}	0.382
		R	15.25^{b}	17.26^{ab}	17.02^{ab}	18.52^{a}	0.304
		FTW	15.25^{b}	18.10^{a}	17.01^{ab}	17.75^{ab}	0.991
		FTR	15.25^{ab}	18.41^{a}	18.32^{a}	18.42^{a}	0.428
		SEM[2)]	-	0.627	0.649	0.634	
	H	A	52.65	51.62	55.41	51.25^{y}	1.931
		I	52.65	47.22	50.92	48.74^{y}	1.655
		R	52.65	48.82	47.00	47.43^{y}	0.832
		FTW	52.65	53.41	56.69	58.85^{x}	1.798
		FTR	52.65^{b}	53.48^{b}	54.82^{b}	59.16^{ax}	0.690
		SEM[2)]	-	1.283	2.205	1.523	
White muscle	CIE L*	A	52.45	56.55	53.17	55.35	1.518
		I	52.45	60.81	51.69	60.11	2.301
		R	52.45^{b}	59.39^{a}	50.91^{b}	59.83^{a}	1.355
		FTW	52.45	58.31	51.11	53.61	2.050
		FTR	52.45^{b}	61.33^{a}	55.23^{ab}	54.16^{b}	1.363
		SEM[2)]	-	2.467	1.077	1.423	
	CIE a*	A	2.91	2.16	4.18^{xy}	1.70^{y}	0.524
		I	2.91^{ab}	1.63^{b}	5.47^{ax}	2.56^{aby}	0.751
		R	2.91^{ab}	1.23^{b}	5.77^{ax}	1.99^{by}	0.417
		FTW	2.91^{ab}	0.87^{b}	4.44^{axy}	1.90 ^{aby}	1.130
		FTR	2.91^{ab}	1.27^{b}	2.73^{aby}	5.61^{ax}	0.724
		SEM[2)]	-	0.428	0.537	0.604	
	CIE b*	A	15.34	16.17^{yz}	15.65^{yz}	16.29^{xy}	0.279
		I	15.34^{ab}	15.42^{abyz}	16.43^{axyz}	14.60^{by}	0.354
		R	15.34	14.50^{z}	15.01^{z}	15.14^{xy}	0.451
		FTW	15.34	16.98^{xy}	16.68^{xy}	15.88^{xy}	0.493
		FTR	15.34^{b}	18.13^{ax}	17.42^{ax}	17.31^{ax}	0.393
		SEM[2)]	-	0.395	0.322	0.506	
	H	A	79.14	83.45	77.85^{xy}	83.99^{x}	1.542
		I	79.14	84.42	71.86^{yz}	80.05^{xy}	2.596
		R	79.14^{ab}	85.15^{a}	69.44^{bz}	82.65^{axy}	1.687
		FTW	79.14	86.74	75.27^{xyz}	83.11^{x}	3.944
		FTR	79.14^{ab}	86.00^{a}	81.57^{abx}	72.19^{bz}	2.172
		SEM[2)]	-	1.488	1.716	2.155	

Dark muscle, brown or reddish tissue on the flesh; white muscle, white to off-white tissue on the flesh.
[1)] n=3 of standard error of the least square mean.
[2)] n=15 of standard error of the least square mean.
[a–c] Different superscripts indicate significant difference among means ($p<0.05$).
[x–z] Different superscripts indicate significant difference among means ($p<0.05$).
A, ambient; I, ice; R, refrigerator; FTW, frozen and thawed in water; FTR, frozen and thawed in a refrigerator; H, hue angle.

values (Listrat et al., 2016). The CIE b* in the dark muscle of fish fillets increased on day 6, except in the FTW and FTR samples, because the freezing condition produced a low TBARS value. The increase in CIE b* of fish fillets is influenced by the escalation of lipid oxidation, which can be assessed using TBARS. This process leads to the generation of reactive oxygen species and accumulation of oxidation products, eventually leading to discoloration and a tougher texture in the muscle tissue (Sriket and La-ongnual, 2018). The results also proved that the FTR and FTW groups had significantly higher hue angles in the dark muscle than the other groups on day 6, which conformed to the relationship between the CIE a* and CIE b* of fish fillets.

Biological and chemical properties

As shown in Fig. 2A, the TBC of mackerel fillets was initially 1.80 Log CFU/g and was significantly higher in group A than in the other groups. Ambient temperature is a favorable environment for microorganism growth and activity (Lee et al., 2014). Theoretically, an increase in microorganism growth simultaneously decreases freshness and initiates spoilage (Mohammed et al., 2021). On day 6, all storage methods were below the acceptable limit of TBC in fish, which was 7 Log CFU/g (ICMSF, 1986; Nayma et al., 2020). However, the A group was not suitable for consumption starting from day 6 due to rapid spoilage, unpleasant odor, and unfavorable quality traits. The FTR group had the lowest TBC during the entire storage period. This is because freezing caused slow growth and/or inactivation of bacteria (Mohammed et al., 2021).

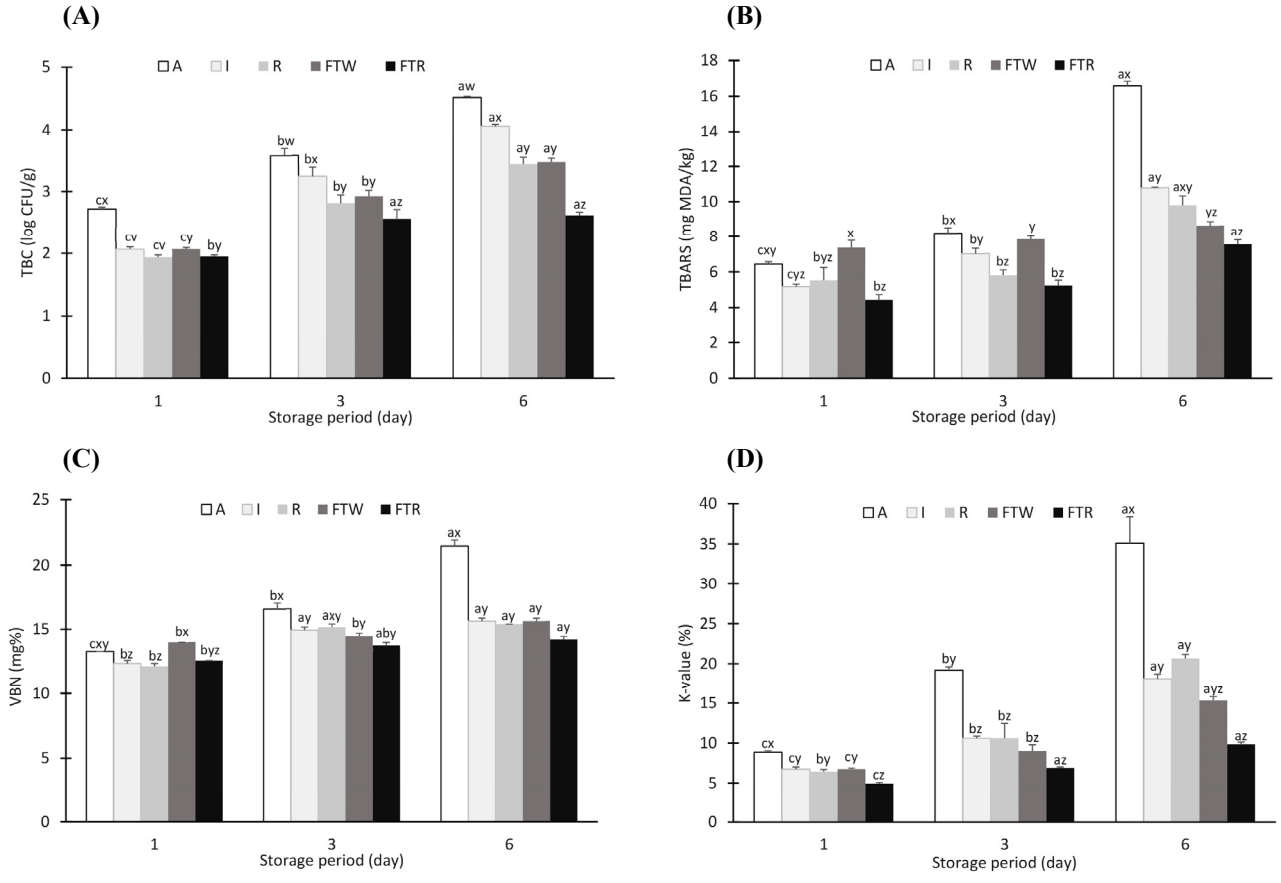

Fig. 2. The total bacterial count (TBC) (A), 2-thiobarbituric acid reactive substance (TBARS) (B), volatile basic nitrogen (VBN) (C) and K-value (D) of mackerel fillets stored under different conditions. $^{a-c}$ Different superscripts represent significant differences among means ($p<0.05$). $^{w-z}$ Different superscripts represent significant differences among means ($p<0.05$). A, ambient; I, ice; R, refrigerator; FTW, frozen and thawed in water; FTR, frozen and thawed in a refrigerator.

Slow lipid oxidation primarily resulting in the formation of hydroperoxide is attributed to the low temperature, which subsequently leads to a gradual increase in lipid autolysis and enzymatic activity in fatty fish (Duarte et al., 2020). Mackerel muscle is highly susceptible to lipid and protein oxidation due to its low post-mortem pH, high polyunsaturated fatty acid content, and abundance of pro-oxidants (Sone et al., 2020). Lipids readily decompose into low-molecular-weight volatile compounds such as aldehydes and ketones, producing unpleasant odors (Domínguez et al., 2019). The initial TBARS value of the mackerel fillets was 3.40 mg malondialdehyde (MDA)/kg. On day 1, the FTW group had the highest TBARS value (7.38 mgMDA/kg) compared to other groups ($p<0.05$) as sown in Fig. 2B, because thawing in water triggered rapid lipid oxidation (Wang and Xie, 2020). However, on day 6, TBARS values were the highest in group A (16.59 mgMDA/kg), followed by I, R, FTW, and FTR groups ($p<0.05$). Ambient temperature can cause massive lipid degradation and peroxidation compared to low temperatures (Domínguez et al., 2019). The FTR group had the lowest TBARS values (4.44–7.56 mgMDA/kg) during the storage period because freezing conditions favored higher disulfide bond content and surface hydrophobicity (Li et al., 2020; Sriket and La-ongnual, 2018).

As stated by Li et al. (2020), decreased enzymatic activity and minimal oxidative reactions during freezing affected the VBN content. The initial VBN value of the samples was 9.10 mg% and it increased linearly with storage time. The FTR group had the lowest VBN values among the different groups ($p<0.05$; Fig. 2C). This is because muscle protein undergoes slow denaturation during storage due to the slow enzymatic reaction, leading to a decrease in soluble proteins (Cropotova et al., 2019). K-value is a parameter based on nucleotide pathways and is used as an indicator of fish flesh freshness. The K-value of mackerel fillets was 8.99% on day 0 and increased continually over the storage period due to the rapid degradation of proteins and lipids. Fish is considered fresh when the K-value is less than 20%, while it is considered spoilt when the K-value exceeds 60% and sensory rejection is initiated at 63% (Mohan et al., 2009; Mohan et al., 2019). Group A had the highest K-value, whereas the FTR samples showed the lowest value during storage ($p<0.05$; Fig. 2D). This finding was similar to that of previous studies where storage at ambient temperature for 6 h elevated the K-values for mullet and pearl spot fishes (Lakshmanan et al., 1996). Turbot stored in cold storage (slurry ice) had a lower K-value than those stored in flake ice (Rodríguez et al., 2006). Tuckey et al. (2010) found justified that the K-value of fish fillets rose rapidly from 19.27% to 52.11% when stored at 15℃ for 36 h.

Physical properties

Textural properties of mackerel fillets stored under different conditions was illustrated in Fig. 3. In general, fish fillets with higher pH have higher water activity, softness, and juiciness (Sun et al., 2018). The decrease in tenderness occurs because of the synergistic effect of numerous endogenous proteolytic systems (Kaur et al., 2021). On day 6, the FTR group showed a hardness and chewiness of 44.06 N and 18.14 N, respectively, which was slightly lower than those (hardness=45.83 N; chewiness=19.57 N) in the FTW group ($p>0.05$). However, the hardness and chewiness of fish fillets in both FTR and FTW groups were significantly lower than those in the other groups, which might be due to microbial proteolysis activity (Matarneh et al., 2017). On day 6, the FTR group had the highest springiness (0.84 mm) among the different storage groups (0.80–0.83 mm; $p>0.05$). Hardness and springiness are common textural indicators of fish freshness, resulting from protein denaturation (Bourne, 2002). Besides, on day 6, the FTR group had the lowest adhesiveness (0.14 kgf.mm) among the different groups (0.17–0.23 kgf.mm). The elasticity increased over the storage period, and on day 6, the FTR group had the highest elasticity (0.03–0.05 Pa) among the different groups. Slower proteolysis due to the low temperature caused fewer changes in protein linkages, maintaining the textural properties (Cropotova et al., 2019).

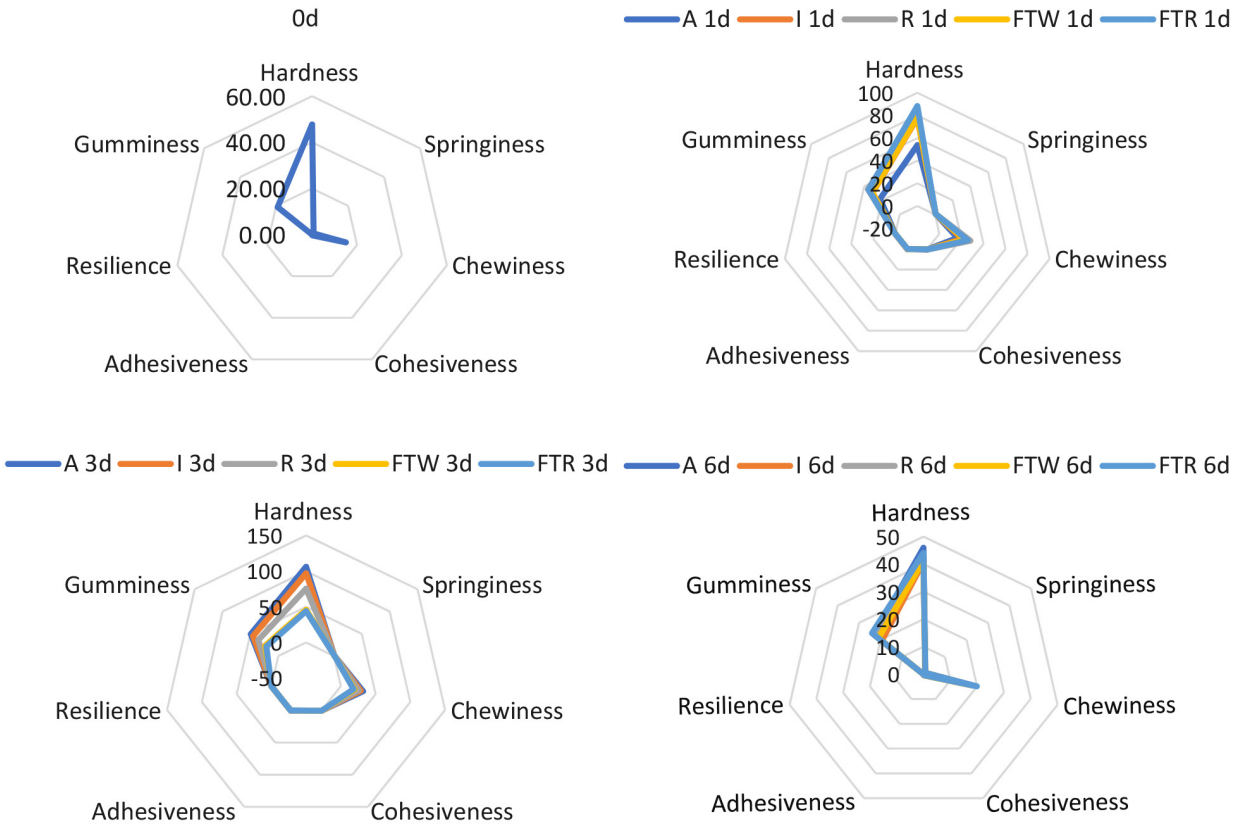

Fig. 3. Textural properties of mackerel fillets stored under different conditions for 0, 1, 3, and 6 days. A, ambient; I, ice; R, refrigerator; FTW, frozen and thawed in water; FTR, frozen and thawed in a refrigerator.

The SEM images of the mackerel fillets stored under different conditions are shown in Fig. 4. Moist environment produces narrowed muscle tissues due to strong muscle contraction (Wang and Xie, 2020). Muscle tissues in mackerel fillets were slightly narrowed in the I and FTW groups on day 1 and were narrower, with more tissue damage on days 3 and 6 compared to the other groups. Shrinkage of muscle tissues at cold temperatures was also observed by Cropotova et al. (2019). The muscle tissues in the FTR group were smooth and elongated, while those in other groups shrunk. SEM observations revealed that group A showed severe structural destruction from day 1 onwards due to high temperature, moist environment, and large muscle contraction (Sigholt et al., 1997). Over the storage period, group I showed less muscle destruction than group A but more muscle destruction than groups FTR and FTW.

Hyperspectral imaging (HSI)-based predictive model

The reflectance spectra before (Fig. 5A) and after pre-processing using wavelength selection (Fig. 5B) and then underwent minimum-maximum normalization (Fig. 5C) were illustrated. Based on the Fig. 6A, it appears that the presence of first and second overtone peaks at 950 and 1,160 nm, respectively, suggests that there are molecular vibrations occurring in the sample that could be associated with O-H stretching bonds by moisture or sulfmyoglobin oxidation (Chen et al., 2021; Khoshnoudi-Nia and Moosavi-Nasab, 2019). Score plots with respect to storage period were used as the reference dataset for PCA as described in Fig. 6B. Spectral data on the quality parameters of the mackerel fillets were obtained using HSI coupled with a PLS-based regression model, as shown in Table 3. PLS showed a relatively high correlation coefficient (R^2_c=0.54–0.96),

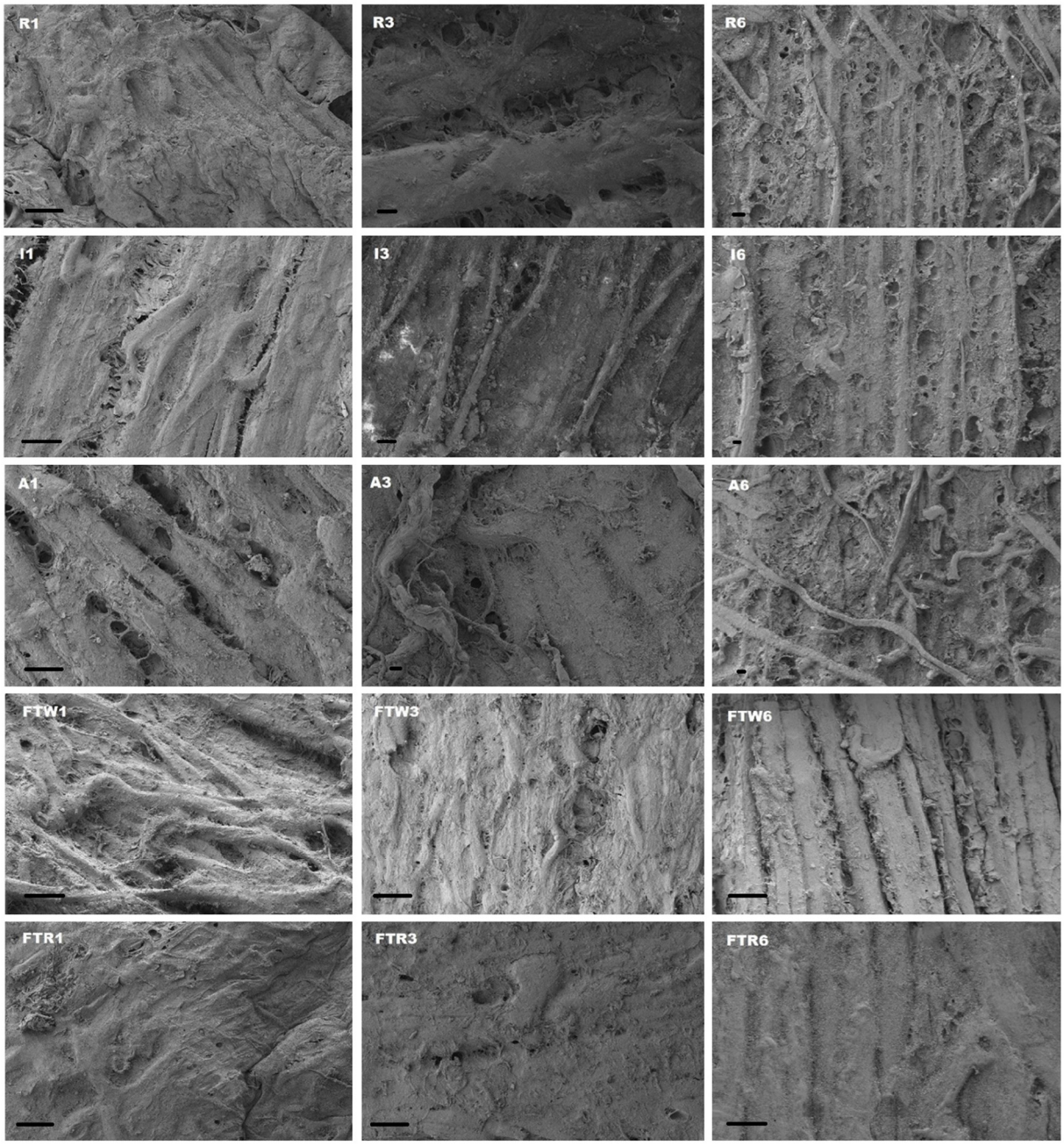

Fig. 4. Scanning electron microscope images of mackerel fillets stored under different conditions during the entire storage period. Scale bar=100 μm. A, ambient; I, ice; R, refrigerator; FTW, frozen and thawed in water; FTR, frozen and thawed in a refrigerator; 1, 1 day; 3, 3 days; 6, 6 days.

which is in agreement with previous studies on muscle foods (Chen et al., 2021; Wu et al., 2016; Xiong et al., 2015; Xu et al., 2016).

The performance of each chemometric model was attributed to the number of samples and variables, type of samples, wavelength range, waveband selection method, and optimal multivariate analysis (Moosavi-Nasab et al., 2021). From the results, 10 of the 17 quality parameters showed good coefficient of correlation in cross-validation values ($R^2_{cv} \geq 0.31$). The remaining had acceptable positive values of R^2_{cv}. However, there is no limitation or acceptable value for R^2 because this value can be improved by modifying the statistical model for the best performance (Temiz and Ulaş, 2021).

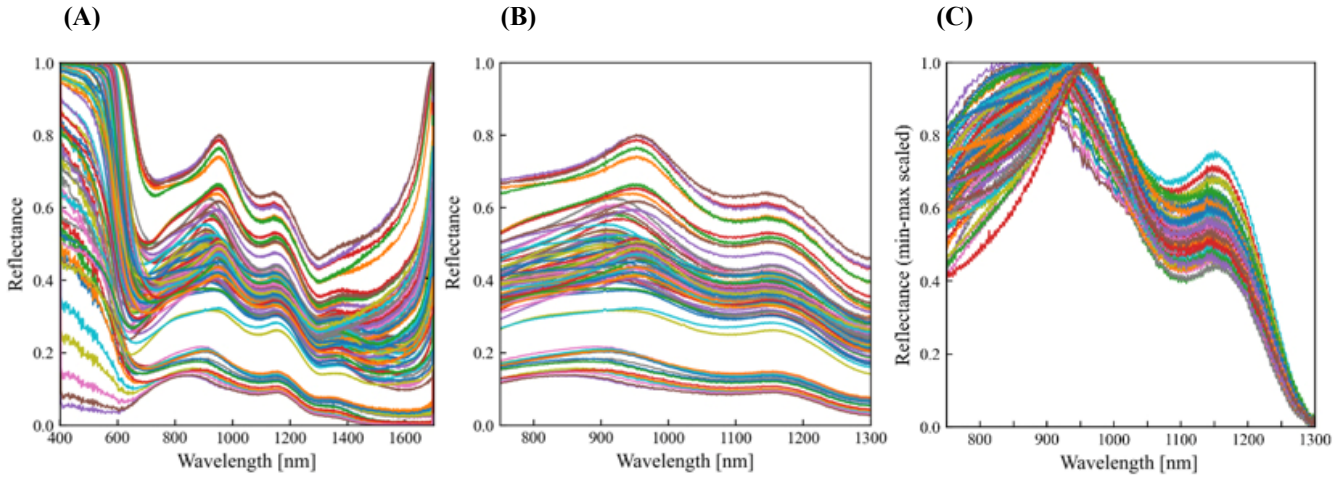

Fig. 5. **The raw data (A), data after wavelength selection (B) and data after wavelength selection and minimum-maximum normalization (C) of reflectance spectra before and after pre-processing.**

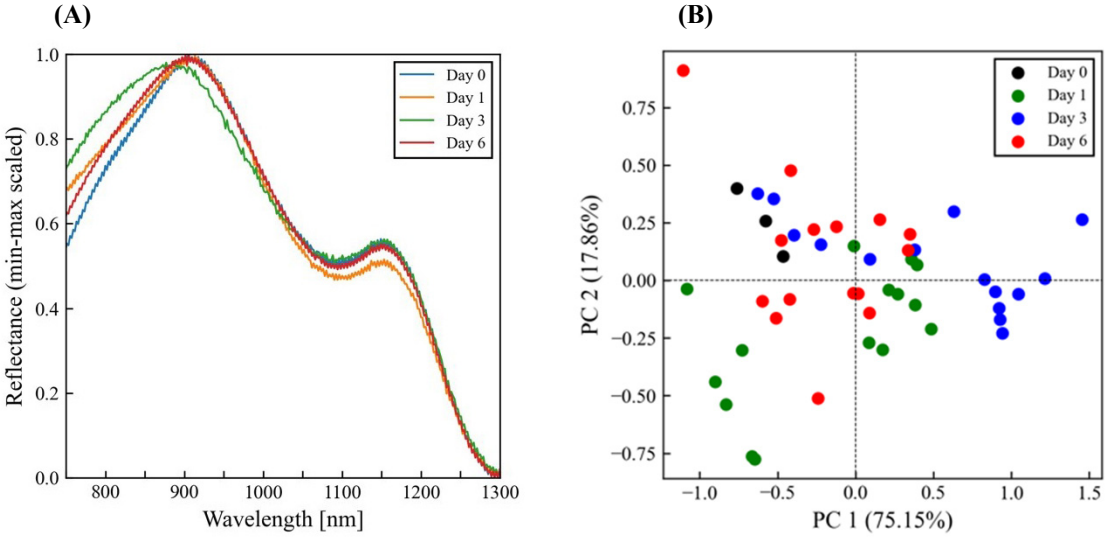

Fig. 6. **Average reflectance (A) and score plots (B) of spectral images throughout the storage period.**

The spectral properties of meat change with pH due to changes in the chemical composition and stretching vibrations of the muscle foods (He et al., 2014). The pH model in this study indicated the highest correlation coefficients for both R^2_{cv} and R^2_c (coefficient of calibration), which were 0.86 and 0.96, respectively, with high PLS components (N=11). For instance, the R^2_c of pH in Atlantic salmon, determined by He et al. (2014), were 0.87 (R^2_{cv}) and 0.89 (R^2_c), which are slightly similar to the current results. Wang et al. (2019) found that the correlation coefficients of pH in crucian carp were 0.72 (R^2_{cv}) and 0.87 (R^2_c). In the present study, VBN obtained using the PLS model had R^2_c=0.87, which was relatively similar to that obtained in other fish fillet studies using PLS and multiple linear regression (MLR; R^2_c=0.76–0.89) and backpropagation – artificial neural network (BP-ANN; R^2_c=0.88; Cheng et al., 2015; Khoshnoudi-Nia and Moosavi-Nasab, 2019; Moosavi-Nasab et al., 2021; Wang et al., 2019).

The TBARS and K-value were also evaluated using the PLS model. Cheng et al. (2016) found more feasible to use PLS, multispectral imaging (MLR), least square-sector vector machine (LS-SVM), genetic algorithms, and successive projection algorithm (SPA) with R^2_{cv}=0.76–0.83. However, the present TBARS values had a slightly lower R^2_{cv} value (0.64) than

Table 3. Partial least square regression model-based calibration and cross-validation results of 17 quality parameters of mackerel fillets measured using hyperspectral imaging during six days of storage

Target	N	Calibration		Cross-validation		
		R^2_C	RMSEC	R^2_{CV}	RMSECV	RPD_{CV}
pH	11	0.96	0.06	0.86	0.12	2.64
Cohesiveness	18	0.99	0.00	0.69	0.03	1.80
TBARS	11	0.91	0.91	0.64	1.83	1.66
Elasticity	12	0.91	0.00	0.63	0.01	1.64
VBN	10	0.87	0.91	0.57	1.67	1.53
K-value	9	0.85	3.05	0.48	5.73	1.39
Hardness	4	0.57	16.19	0.47	17.89	1.38
Springiness	4	0.55	0.04	0.45	0.05	1.35
Dark muscle CIE a*	8	0.74	1.17	0.36	1.86	1.25
White muscle CIE b*	6	0.55	0.79	0.31	0.98	1.20
Dark muscle H	6	0.53	3.09	0.26	3.89	1.16
White muscle CIE a*	6	0.55	1.25	0.19	1.68	1.11
Gumminess	5	0.61	6.57	0.19	9.44	1.11
White muscle CIE L*	5	0.38	3.44	0.17	3.98	1.09
Adhesiveness	3	0.31	0.13	0.16	0.15	1.09
White muscle H	6	0.54	4.18	0.15	5.66	1.09
Chewiness	5	0.54	4.01	0.10	5.64	1.05

N, latent variables; R^2_C, coefficient of calibration; R^2_{cv}, coefficient of cross-validation; RMSEC, root-mean-square errors estimated by calibration; RMSECV, root-mean-square errors estimated by cross-validation; RPD_{CV}, relative percent difference of cross-validation; TBARS, 2-thioabarbituric acid reactive substances; VBN, volatile basic nitrogen; H, hue angle.

aforementioned studies. The TBARS value of frozen-thawed pork was higher when using SPA-PLS (R^2_{cv}=0.80; Wu et al., 2016), while that of chicken meat was higher when using the PLS model (R^2_{cv}=0.87; Xiong et al., 2015). In this study, the K-value was determined at R^2_{cv}=0.48, using the PLS model. Cheng et al. (2015) and Cheng et al. (2016) found that the R^2_{cv} of the K-value in fish fillets was 0.94 using the PLS and LS-SVM models, whereas was 0.95 using the MLR model.

Conclusion

The HSI and conventional analyses revealed that mackerel fillets stored under FTR conditions were the freshest, with minimal impact on physicochemical traits, compared to those kept under other storage conditions. This valuable information had a greater impact on the seafood industry for practical implementation in the short-chain supply before reaching consumers. Interestingly, thawing in the refrigerator was recommended in this study compared to thawing in tap water. The quality of the fish fluctuated with increasing temperature and storage period. The results showed that group A was inappropriate for storing fish fillets. Furthermore, the freshness of the fish fillets in group I was much lower than that of those in the R, FTW, and FTR groups starting from day 3.

The HSI, coupled with the PLS model, yielded positive results for the quality parameters of fish, particularly pH, TBARS, VBN, K-value, and texture. Consequently, the HSI system could replace the conventional method for evaluating the quality

of fish fillets, reducing analysis time and costs. These findings provided valuable insights into the potential and effectiveness of using HSI in fundamental applications within the seafood industry. A comprehensive understanding of storage design for fish fillets could enable the industry to employ the best methods for maintaining fish quality.

The practical application in these studies undoubtedly offers significant knowledge to the seafood industry regarding the storage of fish fillets and the use of HSI as a non-destructive quality measurement tool. The HSI results for quality parameters using the PLS model could be improved by employing reliable multivariate analyses to achieve higher correlation coefficients and accuracy compared to the presented results. Further studies measuring metabolite contents in fish fillets using the HSI system are recommended to confirm its effectiveness and efficiency in analyzing low-molecular-weight compounds.

Conflicts of Interest

The authors declare no potential conflicts of interest.

Acknowledgements

This work was supported by Korea Institute of Planning and Evaluation for Technology in Food, Agriculture and Forestry (IPET) through Smart Agri Products Flow Storage Technology Development Program, funded by Ministry of Agriculture, Food and Rural Affairs (MAFRA) (1545027072); and the National Research Foundation of Korea (NRF) grant funded by the Korean government (MSIT), grant number NRF-2020M3C1C1A01084648.

Author Contributions

Conceptualization: Ismail A, Jo C. Data curation: Yim DG. Formal analysis: Ismail A, Ryu J. Methodology: Ryu J, Kim SS, Lee HJ. Software: Ismail A, Ryu J, Kim G. Validation: Yim DG, Kim G. Investigation: Ismail A, Kim SS, Lee HJ. Writing - original draft: Ismail A. Writing - review & editing: Ismail A, Ryu J, Yim DG, Kim G, Kim SS, Lee HJ, Jo C.

Ethics Approval

This article does not require IRB/IACUC approval because there are no human and animal participants.

References

Andrés SC, García ME, Zaritzky NE, Califano AN. 2006. Storage stability of low-fat chicken sausages. J Food Eng 72:311-319.

Bourne MC. 2002. Principles of objective texture measurement. In Food texture and viscosity: Concept and measurement. 2nd ed. Bourne MC (ed). Academic Press, San Diego, CA, USA. pp 107-188.

Brewer MS. 2014. Chemical and physical characteristics of meat: Water-holding capacity. In Encyclopedia of meat sciences. 2nd ed. Dikeman M, Devine C (ed). Academic Press, San Diego, CA, USA. pp 274-282.

Chan SS, Roth B, Skare M, Hernar M, Jessen F, Løvdal T, Jakobsen AN, Lerfall J. 2020. Effect of chilling technologies on water holding properties and other quality parameters throughout the whole value chain: From whole fish to cold-smoked

fillets of Atlantic salmon (*Salmo salar*). Aquaculture 526:735381.

Chen Z, Wang Q, Zhang H, Nie P. 2021. Hyperspectral imaging (HSI) technology for the non-destructive freshness assessment of pearl gentian grouper under different storage conditions. Sensors 21:583.

Cheng JH, Sun DW, Pu HB, Zhu Z. 2015. Development of hyperspectral imaging coupled with chemometric analysis to monitor K value for evaluation of chemical spoilage in fish fillets. Food Chem 185:245-253.

Cheng JH, Sun DW, Qu JH, Pu HB, Zhang XC, Song Z, Chen X, Zhang H. 2016. Developing a multispectral imaging for simultaneous prediction of freshness indicators during chemical spoilage of grass carp fish fillet. J Food Eng 182:9-17.

Cheng JH, Sun DW, Wei Q. 2017. Enhancing visible and near-infrared hyperspectral imaging prediction of TVB-N level for fish fillet freshness evaluation by filtering optimal variables. Food Anal Methods 10:1888-1898.

Conway EJ. 1947. Microdiffusion analysis and volumetric error. Crosby Lockwood & Son, London, UK. p 357.

Cropotova J, Mozuraityte R, Standal IB, Grøvlen MS, Rustad T. 2019. Superchilled, chilled and frozen storage of Atlantic mackerel (*Scomber scombrus*) fillets: Changes in texture, drip loss, protein solubility and oxidation. Int J Food Sci Technol 54:2228-2235.

Domínguez R, Pateiro M, Gagaoua M, Barba FJ, Zhang W, Lorenzo JM. 2019. A comprehensive review on lipid oxidation in meat and meat products. Antioxidants 8:429.

Duarte AM, Silva F, Pinto FR, Barroso S, Gil MM. 2020. Quality assessment of chilled and frozen fish: Mini review. Foods 9:1739.

Govari M, Tryfinopoulou P, Parlapani FF, Boziaris IS, Panagou EZ, Nychas GJE. 2021. Quest of intelligent research tools for rapid evaluation of fish quality: FTIR spectroscopy and multispectral imaging versus microbiological analysis. Foods 10:264.

Greer GG. 2020. Red meats, poultry, and fish. In Enzymes of psychrotrophs in raw food. McKellar RC (ed). CRC Press, Boca Raton, FL, USA. pp 267-292.

Hashimoto K, Kobayashi S, Yamashita M. 2017. Comparison of connective tissue structure and muscle toughness of spotted mackerel *Scomber australasicus* and Pacific mackerel *S. japonicus* during chilled and frozen storage. Fish Sci 83:133-139.

Hassoun A, Karoui R. 2017. Quality evaluation of fish and other seafood by traditional and nondestructive instrumental methods: Advantages and limitations. Crit Rev Food Sci Nutr 57:1976-1998.

Hassoun A, Shumilina E, Di Donato F, Foschi M, Simal-Gandara J, Biancolillo A. 2020. Emerging techniques for differentiation of fresh and frozen–thawed seafoods: Highlighting the potential of spectroscopic techniques. Molecules 25:4472.

He HJ, Wu D, Sun DW. 2014. Rapid and non-destructive determination of drip loss and pH distribution in farmed Atlantic salmon (*Salmo salar*) fillets using visible and near-infrared (Vis–NIR) hyperspectral imaging. Food Chem 156:394-401.

Huang YZ, Liu Y, Jin Z, Cheng Q, Qian M, Zhu BW, Dong XP. 2021. Sensory evaluation of fresh/frozen mackerel products: A review. Compr Rev Food Sci Food Saf 20:3504-3530.

International Commission on Microbiological Specifications for Foods [ICMSF]. 1986. Microorganisms in foods 2. Sampling for microbiological analysis: Principles and specific applications. 2nd ed. Blackwell Scientific Publications, Oxford, UK. p 310.

Kaur L, Hui SX, Morton JD, Kaur R, Chian FM, Boland M. 2021. Endogenous proteolytic systems and meat tenderness: Influence of post-mortem storage and processing. Food Sci Anim Resour 41:589-607.

Khoshnoudi-Nia S, Moosavi-Nasab M. 2019. Prediction of various freshness indicators in fish fillets by one multispectral

imaging system. Sci Rep 9:14704.

Lakshmanan PT, Antony PD, Gopakumar K. 1996. Nucleotide degradation and quality changes in mullet (*Liza corsula*) and pearlspot (*Etroplus suratensis*) in ice and at ambient temperatures. Food Control 7:277-283.

Lee H, Yong HI, Kim HJ, Choe W, Yoo SJ, Jang EJ, Jo C. 2016. Evaluation of the microbiological safety, quality changes, and genotoxicity of chicken breast treated with flexible thin-layer dielectric barrier discharge plasma. Food Sci Biotechnol 25:1189-1195.

Lee SH, Jung JY, Jeon CO. 2014. Effects of temperature on microbial succession and metabolite change during saeu-jeot fermentation. Food Microbiol 38:16-25.

Li D, Zhao H, Muhammad AI, Song L, Guo M, Liu D. 2020. The comparison of ultrasound-assisted thawing, air thawing and water immersion thawing on the quality of slow/fast freezing bighead carp (*Aristichthys nobilis*) fillets. Food Chem 320:126614.

Listrat A, Lebret B, Louveau I, Astruc T, Bonnet M, Lefaucheur L, Picard B, Bugeon J. 2016. How muscle structure and composition influence meat and flesh quality. Sci World J 2016:3182746.

Liu D, Eng XA, Sun DW. 2013. NIR spectroscopy and imaging techniques for evaluation of fish quality: A review. Appl Spectrosc Rev 48:609-628.

Magnussen OM, Haugland A, Hemmingsen AKT, Johansen S, Nordtvedt TS. 2008. Advances in superchilling of food: Process characteristics and product quality. Trends Food Sci Technol 19:418-424.

Matarneh SK, England EM, Scheffler TL, Gerrard DE. 2017. The conversion of muscle to meat. In Lawrie's meat science. 8th ed. Toldrá F (ed). Woodhead, Cambridge, UK. pp 159-185.

Mohammed HHH, He L, Nawaz A, Jin G, Huang X, Ma M, Abdegadir WS, Elgasim EA, Khalifa I. 2021. Effect of frozen and refrozen storage of beef and chicken meats on inoculated microorganisms and meat quality. Meat Sci 175:108453.

Mohan CO, Ravishankar CN, Ashok Kumar K, Srinivasa Gopal TK. 2019. Biogenic amines and nucleotide breakdown products of sodium acetate, sodium lactate, and sodium citrate treated seer fish (*Scomberomorus commerson*) during iced storage. J Food Saf 39:e12633.

Mohan CO, Ravishankar CN, Srinivasa Gopal TK, Ashok Kumar K. 2009. Nucleotide breakdown products of seer fish (*Scomberomorus commerson*) steaks stored in O_2 scavenger packs during chilled storage. Innov Food Sci Emerg Technol 10:272-278.

Moosavi-Nasab M, Khoshnoudi-Nia S, Azimifar Z, Kamyab S. 2021. Evaluation of the total volatile basic nitrogen (TVB-N) content in fish fillets using hyperspectral imaging coupled with deep learning neural network and meta-analysis. Sci Rep 11:5094.

Nayma K, Das KC, Alice EJ, Mehbub MF, Islam MT. 2020. Extension of shelf-life of ready-to-cook (RTC) pangas fish (*Pangasianodon hypophthalmus*) curry by modified atmosphere packaging at chilled storage. IOP Conf Ser Earth Environ Sci 414:012015.

Negara BFSP, Kim SR, Sohn JH, Kim JS, Choi JS. 2021. Application of high-frequency defrosting, superheated steam, and quick-freezing treatments to improve the quality of seafood home meal replacement products consisting of the adductor muscle of pen shells and common squid meat. Appl Sci 11:2926.

Prabhakar PK, Vatsa S, Srivastav PP, Pathak SS. 2020. A comprehensive review on freshness of fish and assessment: Analytical methods and recent innovations. Food Res Int 133:109157.

Rodríguez Ó, Barros-Velázquez J, Piñeiro C, Gallardo JM, Aubourg SP. 2006. Effects of storage in slurry ice on the

microbial, chemical and sensory quality and on the shelf life of farmed turbot (*Psetta maxima*). Food Chem 95:270-278.

Roiha IS, Jónsson Á, Backi CJ, Lunestad BT, Karlsdóttir MG. 2018. A comparative study of quality and safety of Atlantic cod (*Gadus morhua*) fillets during cold storage, as affected by different thawing methods of pre-rigor frozen headed and gutted fish. J Sci Food Agric 98:400-409.

Sigholt T, Erikson U, Rustad T, Johansen S, Nordtvedt TS, Seland A. 1997. Handling stress and storage temperature affect meat quality of farmed-raised Atlantic salmon (*Salmo Salar*). J Food Sci 62:898-905.

Singh A, Benjakul S. 2018. Proteolysis and its control using protease inhibitors in fish and fish products: A review. Compr Rev Food Sci Food Saf 17:496-509.

Sone I, Sveinsdóttir HI, Stefánsson G, Larsson K, Undeland I, Skåra T, Romotowska PE, Karlsdóttir MG. 2020. Investigating commercially relevant packaging solutions to improve storage stability of mechanically filleted Atlantic mackerel (*Scomber scombrus*) produced under industrial conditions. Eur Food Res Technol 246:693-701.

Sriket P, La-ongnual T. 2018. Quality changes and discoloration of basa (*Pangasius bocourti*) fillet during frozen storage. J Chem 2018:5159080.

Sun Y, Ma L, Ma M, Zheng H, Zhang X, Cai L, Li J, Zhang Y. 2018. Texture characteristics of chilled prepared mandarin fish (*Siniperca chuatsi*) during storage. Int J Food Prop 21:242-254.

Tan M, Mei J, Xie J. 2021. The formation and control of ice crystal and its impact on the quality of frozen aquatic products: A review. Crystals 11:68.

Temiz HT, Ulaş B. 2021. A review of recent studies employing hyperspectral imaging for the determination of food adulteration. Photochem 1:125-146.

Toe CJ, Foo HL, Loh TC, Mohamad R, Abdul Rahim R, Idrus Z. 2019. Extracellular proteolytic activity and amino acid production by lactic acid bacteria isolated from Malaysian foods. Int J Mol Sci 20:1777.

Tuckey NPL, Forster ME, Gieseg SP. 2010. Effects of rested harvesting on muscle metabolite concentrations and K-values in Chinook salmon (*Oncorhynchus tshawytscha*) fillets during storage at 15°C. J Food Sci 75:C459-C464.

Wang X, Russel M, Zhang Y, Zhao J, Zhang Y, Shan J. 2019. A clustering-based partial least squares method for improving the freshness prediction model of crucian carps fillets by hyperspectral image technology. Food Anal Methods 12:1988-1997.

Wang X, Xie J. 2020. Effects of different thawing methods on the quality of frozen horse mackerel. Shipin Kexue 41:137-143.

Wu T, Ge Y, Li Y, Xiang Y, Jiang Y, Hu Y. 2018. Quality enhancement of large yellow croaker treated with edible coatings based on chitosan and lysozyme. Int J Biol Macromol 120:1072-1079.

Wu X, Song X, Qiu Z, He Y. 2016. Mapping of TBARS distribution in frozen–thawed pork using NIR hyperspectral imaging. Meat Sci 113:92-96.

Xiong Z, Sun DW, Pu H, Xie A, Han Z, Luo M. 2015. Non-destructive prediction of thiobarbituric acid reactive substances (TBARS) value for freshness evaluation of chicken meat using hyperspectral imaging. Food Chem 179:175-181.

Xu JL, Riccioli C, Sun DW. 2016. Development of an alternative technique for rapid and accurate determination of fish caloric density based on hyperspectral imaging. J Food Eng 190:185-194.

Xu L, Hu O, Guo Y, Zhang M, Lu D, Cai CB, Xie S, Goodarzi M, Fu HY, She YB. 2018. Representative splitting cross validation. Chemometr Intell Lab Syst 183:29-35.

Zhang Y, Li S, Jin S, Li F, Tang J, Jiao Y. 2021. Radio frequency tempering multiple layers of frozen tilapia fillets: The

temperature distribution, energy consumption, and quality. Innov Food Sci Emerg Technol 68:102603.

Zhou P, Xie J. 2021. Effect of different thawing methods on the quality of mackerel (*Pneumatophorus japonicus*). Food Sci Biotechnol 30:1213-1223.

Zhou X, Yu X, Xie F, Fan Y, Xu X, Qi J, Xiong G, Gao X, Zhang F. 2021. pH-responsive double-layer indicator films based on konjac glucomannan/camellia oil and carrageenan/anthocyanin/curcumin for monitoring meat freshness. Food Hydrocoll 118:106695.